

1 **Operational forecast framework applied to extreme sea levels at regional and**
2 **local scales**

3 **André B. Fortunato^{1,*}; Anabela Oliveira^{2,*}; João Rogeiro³; Ricardo Tavares da Costa⁴; João L.**
4 **Gomes⁵; Kai Li⁶; Gonçalo de Jesus⁷; Paula Freire⁸; Ana Rilo⁹; Ana Mendes¹⁰; Marta Rodrigues¹¹;**
5 **Alberto Azevedo¹²**

6 **Submitted to Journal of Operational Oceanography, March, 2016**

7 **Reviewed, October, 2016**

8 **Available online: November 22, 2016**

9 **Please cite as:** Fortunato A.B., Oliveira A., Rogeiro J., Tavares da Costa R., Gomes J.L., Li K., Jesus G.,
10 Freire P., Rilo A., Mendes A., Rodrigues M., Azevedo A. (2017). Operational forecast framework applied
11 to extreme sea levels at regional and local scales, *Journal of Operational Oceanography*, 10/1: 1-15, DOI:
12 10.1080/1755876X.2016.1255471

1 ¹ Estuarine and Coastal Zones Unit, National Civil Engineering Laboratory, Av. do Brasil 101, 1700-066 Lisbon, Portugal, afortunato@lnec.pt. Corresponding author

2 ² Information Technology in Water and Environment Research Group, National Civil Engineering Laboratory, Av. do Brasil 101, 1700-066 Lisbon, Portugal, aoliveira@lnec.pt

3 ³ Information Technology in Water and Environment Research Group, National Civil Engineering Laboratory, Av. do Brasil 101, 1700-066 Lisbon, Portugal, jrogeiro@lnec.pt

4 ⁴ Estuarine and Coastal Zones Unit, National Civil Engineering Laboratory, Av. do Brasil 101, 1700-066 Lisbon, Portugal, rcosta@lnec.pt

5 ⁵ Information Technology in Water and Environment Research Group, National Civil Engineering Laboratory, Av. do Brasil 101, 1700-066 Lisbon, Portugal, jlgomes.web@gmail.com

6 ⁶ Formerly at National Civil Engineering Laboratory, Av. do Brasil 101, 1700-066 Lisbon, Portugal. Now at Sun Yat-sen University, China, likai28@sysu.edu.cn.

7 ⁷ Information Technology in Water and Environment Research Group, National Civil Engineering Laboratory, Av. do Brasil 101, 1700-066 Lisbon, Portugal, gjesus@lnec.pt

8 ⁸ Estuarine and Coastal Zones Unit, National Civil Engineering Laboratory, Av. do Brasil 101, 1700-066 Lisbon, Portugal, pfreire@lnec.pt

9 ⁹ Estuarine and Coastal Zones Unit, National Civil Engineering Laboratory, Av. do Brasil 101, 1700-066 Lisbon, Portugal, arilo@lnec.pt

10 ¹⁰ Information Technology in Water and Environment Research Group, National Civil Engineering Laboratory, Av. do Brasil 101, 1700-066 Lisbon, Portugal, amendes@lnec.pt

11 ¹¹ Estuarine and Coastal Zones Unit, National Civil Engineering Laboratory, Av. do Brasil 101, 1700-066 Lisbon, Portugal, mfrdrigues@lnec.pt

12 ¹² Estuarine and Coastal Zones Unit, National Civil Engineering Laboratory, Av. do Brasil 101, 1700-066 Lisbon, Portugal, aazevedo@lnec.pt

* Both authors contributed equally to this work

14 **ACKNOWLEDGEMENT**

15 This work was partially supported by the Fundação para a Ciência e a Tecnologia, through
16 project MOLINES (PTDC/AAG-MAA/2811/2012) and three grants (M. Rodrigues:
17 SFRH/BPD/87512/2012; A. Azevedo: SFRH/BPD/73089/2010; G. Jesus:
18 SFRH/BD/82489/2011).

19

20 **Abstract**

21 The design, implementation and demonstration of a novel and generic computational forecast
22 framework for multi-scale prediction of extreme sea levels and associated flooding is presented.
23 Denoted Water Information Forecast Framework (WIFF), it integrates process-based models for
24 waves, tides and surges from regional to local scales, predicting the flooding of coastal areas, and
25 supporting the routine and emergency management of coastal resources. WIFF manages the
26 simulations and the real-time monitoring data, archives the data and makes the information
27 available through a WebGIS that targets users with distinct access privileges. Additionally, the
28 web component of WIFF adapts automatically and transparently to any device. WIFF also
29 provides ways to assess the model accuracy and generates tailored products based on model
30 results and observations. WIFF is demonstrated in the prediction of extreme water levels in the
31 Portuguese coast, simulating processes at different scales: at basin scales, waves are simulated in
32 the North Atlantic and in the Portuguese shelf, and sea levels due to tides and atmospheric
33 forcings are simulated in the North-east Atlantic; at estuarine scales, high-resolution, fully
34 coupled wave/circulation predictions are performed in the Tagus estuary to account for wave-
35 current interactions. User-oriented georeferenced products are generated, including automatic
36 model/data comparisons, targeting the needs of civil protection agents and combining for the first
37 time an agile, service-oriented platform with high-resolution, process-rich predictions of the
38 Tagus dynamics.

39 **Keywords:** Forecast systems; WebGIS; real-time information framework; Portuguese shelf;
40 Tagus estuary; storm surge.

41 **1. Introduction**

42 Many coastal zones in the world are at a high risk of flooding. On the one hand, these areas are
43 usually densely populated, hence particularly vulnerable to extreme events; on the other hand,
44 coastal areas are often low-lying lands, exposed to tides, storm surges and waves. Climate change
45 further aggravates the flood hazard through sea level rise and the increase of the intensity and

46 frequency of extreme events. This risk is illustrated by several catastrophic events in the last
47 decade, such as the 2005 hurricane Katrina (Dietrich et al. 2011), and the 2010 Xynthia (Bertin et
48 al. 2012; Liberato et al. 2013), and 2014 Hercules (Castelle et al. 2015) storms.

49 Waves, tides and surges have been successfully simulated in the past few decades using process-
50 based models (e.g. Dodet et al. 2010, Dietrich et al. 2011, Bertin et al. 2012), taking advantage of
51 increasingly faster computational resources. In recent years, the need to provide the information
52 required to initiate preventive and emergency actions has triggered the development of dedicated
53 forecast systems to predict the occurrence of extreme events (Bajo and Umgiesser 2010;
54 Dresback et al. 2013, Zhang et al. 2013, Gallien et al. 2013). As coastal flooding events typically
55 result from large-scale phenomena propagating from the ocean to localized coastal areas, a
56 modeling approach that covers multiple spatial scales and distinct processes is required. As a
57 result, the large computational resources necessary to provide accurate and timely early-warnings
58 of extreme events have fostered the use of high-performance computing (HPC) environments,
59 such as computer clusters (Ramakrishnan et al. 2006; Rogeiro et al. 2015).

60 Recent developments in Information Technology (IT), such as communication networks,
61 Geographic Information Systems (GIS) and decision support systems, are also enhancing disaster
62 management and communications. In recent years, many web-based emergency response systems
63 have been developed (e.g., the Global Disaster Alert and Coordination System,
64 <http://www.gdacs.org/>; and the Global Disaster Information Network <http://www.gdin.org>) with
65 increasingly complex designs (Kyng et al. 2006). Other examples with complex software
66 architectures, integrating GIS, web-based spatial databases (Herold et al. 2005) and providing
67 authenticated users access to targeted information on-demand (Kulkarni et al. 2014), have also
68 been proposed. IT solutions integrating process-based models have therefore an enormous
69 potential to transform coastal zone management by providing accurate and autonomously updated
70 information. In particular, web platforms combining multiple access levels to different hierarchic
71 roles, with the capacity to adapt to specific use cases without significant code changes, constitute
72 a major contribution to sustainable coastal zone management, and will probably continue to
73 evolve in the near future (Gomes et al. 2015).

74 Forecast information systems are fundamental components of emergency response systems. They
75 are now emerging as operational tools for the management of harbors and marine resources
76 (Daniel et al. 2004; Baptista 2006, Anselmi-Molina et al. 2012; Chandrasekar et al. 2012;
77 Wernera et al. 2013), by providing precise and timely predictions on water conditions. Forecast
78 systems integrate remote monitoring networks, HPC resources (due to demanding computation
79 processes), either for short-term forecasting or resulting data processing, and web-based
80 information systems to support management decisions (Baptista et al. 2015).

81 The balance between the need to provide timely alerts and the adequate spatial and temporal
82 resolution for reliable water predictions motivates the search for an optimal forecast setup, from
83 both modeling and infrastructures viewpoints. Besides adequate water process representation,
84 computational requirements for water forecasts include the need to scale up to multiple spatial
85 scales and the time for forecasts to be available.

86 Building on these experiences, a web-accessible framework denoted as WIFF (Water Information
87 Forecast Framework) has recently been developed to provide access to real-time observations and
88 model predictions to decision-makers, constituting at the same time a repository of historical
89 information (Jesus et al. 2012, Oliveira et al. 2014). Herein, this concept is extended to flood
90 forecasting, seamlessly integrating high-resolution models across processes (waves, tides, storm
91 surges) and spatial scales (from regional to local), combined with an innovative, responsive, real-
92 time information web interface for enhanced support to flood risk emergency in estuarine areas,
93 targeting multiple users with distinct access privileges.

94 The framework is demonstrated in the integrated prediction of extreme water levels in the
95 Portuguese coast and the Tagus estuary. The primary aim of this deployment is to provide the
96 civil protection authorities with all the information required to anticipate and react to flood events
97 along the margins of the Tagus estuary, focusing on flooding originating from the sea. Besides
98 the forecast platform described herein, additional information such as vulnerability and risk
99 indexes were also implemented in the WIFF WebGIS interface (Tavares et al. 2015, Gomes et al.
100 2015).

101 This paper is organized as follows. The generic computational forecast framework is described
102 first, including the requirements, the infrastructure and the technological choices for the WebGIS
103 interface. The functionalities of the framework are then illustrated through an application to the
104 Portuguese coast. The deployment involves the implementation and validation of the operational
105 models: a regional wave model of the North Atlantic with a nested grid on the Portuguese shelf, a
106 tide and surge model of the Northeast Atlantic, and a coupled wave-circulation model of the
107 Tagus estuary. Finally, some challenges associated with this type of systems are discussed.

108 **2. Methodology and implementation**

109 ***2.1. Requirements***

110 The real-time information forecast framework WIFF aims to support flood risk management in
111 coastal areas, targeting multiple users with distinct access privileges. Therefore, its
112 conceptualization was based on a user's requirements analysis targeting all potential users and
113 purposes. The following user requirements were identified:

- 114 • web access to relevant georeferenced information from wireless sensors, high-resolution
115 forecasts and comprehensive risk analysis;
- 116 • fast and automatic adaptation to different devices;
- 117 • user-dependent access to data and products;
- 118 • portability to other coastal and urban systems.

119 The next two sub-sections present the framework's overall architecture and the forecast modeling
120 infrastructure.

121 ***2.2. The Water Information Forecast Framework***

122 WIFF aims to provide on-line, intuitive and georeferenced access to real-time observations and
123 model predictions, as well as on-demand services in support of routine management of coastal
124 resources and harbor operations. Simultaneously, WIFF provides a repository of historical
125 information, available at each deployment site to the relevant end-users. Originally conceived for

126 a single user type, the WIFF's WebGIS now allows for users with different access privileges,
127 following the requirement analysis summarized above.

128 The framework is composed by two distinct parts (Figure 1): the back-end, executed by the
129 server, runs the simulations and retrieves, processes and stores the observations and the model
130 results; the front-end, executed by the client's browser, interacts with the end-user and displays
131 the information made available by the back-end. The client-server architecture enforces the
132 separation of concerns in the two components of the system, making them simpler and more
133 robust since each one only has to worry about its own duties. Also, each component can be
134 replaced and developed independently, as long as the interface between them is not altered. This
135 interface uses Representational State Transfer (REST) web-services, a set of principles which
136 separates the communication protocols from the interaction between clients and servers. The
137 replies to the requests from the front-end to the back-end are wrapped in JavaScript Object
138 Notation (JSON), a format to exchange information that is easy to read and write by humans and
139 easy to analyze by computers.

140 [Figure 1 near here]

141 The back-end is composed by a deployment of CakePHP, a Model-view-controller PHP
142 framework. It has a PostgreSQL database, using PostGIS extension to interpret geographical
143 data, coupled with several instances of GeoServer, and some Perl and Python scripts. The PHP
144 code manages the control and user access to the data delivered to the front-end and connects the
145 different components of the back-end. The GeoServer, an open source map server that allows
146 users to publish geospatial information using open standards, manages and delivers
147 georeferenced images in normalized formats (e.g., Web Map Service – WMS), so that this
148 information can easily be used by different clients. This geospatial map server offers vector and
149 timed data, stored in PostgreSQL/PostGIS databases and in shapefile format files, thereby
150 allowing the exploitation of the model results in great detail (e.g., through the extraction of time
151 series in selected points by the user in the WebGIS interface or the display of non-pixelated
152 layers).

153 The front-end consists of a web application, adaptable to different types of devices, which allows
154 the user to visualize and interact with the results made available by the back-end in a simple and
155 intuitive interface. The adaptation of the platform to devices with a lower processing capability,
156 such as smartphones and tablets, requires the use of efficient web technologies: HTML5 and
157 CSS3, the bases of all modern web applications; AngularJS, a javascript framework that offers a
158 templating and two-way data binding dynamic system; Google Polymer, an implementation of
159 visual design patterns; and OpenLayers, a library that allows the manipulation of georeferenced
160 information and supplies tools to handle maps from the client side.

161 Because emergency response requires swift decisions, the rapid display of information to the end-
162 users is a stringent requirement for forecast systems such as WIFF. To address this requirement
163 with limited computational resources, WIFF's GeoServer caches all map layers, through an
164 integrated GeoWebCache, coupled with pre-seeding of the content at the moment of its creation.
165 This approach allows the server to have the content already rendered, ready to be delivered to the
166 user with minimal CPU usage. GeoWebCache is a Java web application used to cache map tiles
167 coming from a variety of sources, such as OGC Web Map Service (WMS) compliant servers
168 (such as the GeoServer). It implements various service interfaces (such as WMS-C, WMTS,
169 TMS, Google Maps KML, Virtual Earth) in order to accelerate and optimize map image delivery.
170 It runs as a proxy between a map client application and a map server, caching (storing) tiles on-
171 demand or pre-seeded, eliminating redundant request processing and thus drastically reducing
172 processing time.

173 ***2.3. Modeling infrastructure***

174 The forecast modeling infrastructure used herein originated from the Rapid Deployment Forecast
175 System (RDFS – Baptista 2006), a generic forecasting platform, adaptable to any geographical
176 location. The original RDFS was extended to water quality (David et al. 2013) and waves,
177 integrated in a WebGIS tailored for coastal applications (Jesus et al. 2012) and extended to risk
178 analysis (Oliveira et al. 2014). The forecast system integrates a set of wave, circulation and water
179 quality models that run periodically in HPC environments to generate forecasts of water levels,

180 currents, water temperatures, salinity, waves and selected water quality indicators for target areas.
181 For the particular case of flooding, only wave and circulation models are used.

182 While flooding occurs at small spatial scales, its triggering events can be generated in large
183 oceanic basins. Regional scale models are thus required to adequately reproduce the processes
184 that will eventually cause flooding (e.g., Blain et al. 1994): the generation and propagation of
185 waves, tides and storm surges. Hence, these processes must first be simulated at basin scales, to
186 provide boundary conditions for local, coastal models. In deep areas, the non-linear interaction
187 between long (tides and surges) and short (surface) waves can generally be neglected, allowing
188 the two processes to be simulated independently. In contrast, wave propagation is affected by
189 tidal currents and water level fluctuations in shallow areas, and wave breaking can generate
190 significant currents and elevation setup at the coast. This setup can propagate far inside estuaries,
191 thereby affecting the total water levels. For instance, Fortunato et al. (2016b) showed that during
192 a major storm, the wave setup reached about 0.5 m inside the Tagus estuary. Hence, tidal and
193 wave dynamics in coastal areas should be simulated with coupled models that compute all the
194 relevant physical processes and their interactions simultaneously.

195 Herein WIFF was extended to account for these interactions, integrating a coupled model for
196 wave and currents. The forecast modeling system uses therefore different models at different
197 scales. First, waves, tides and surges forecasts are produced at regional scales. The wave fields
198 are generated with the third generation spectral wave model WAVEWATCH III (Tolman, 2009),
199 allowing for several levels of nesting to accommodate the necessary grid resolution. Sea surface
200 elevations are simulated at a regional scale using the shallow water model SCHISM (Semi-
201 implicit Cross-scale Hydroscience Integrated System Model – Zhang et al. 2016). Derived from
202 SELFE (Zhang and Baptista 2008), SCHISM is an open-source community-supported modelling
203 system based on unstructured grids, designed for the seamless simulation of 3D baroclinic
204 circulation across lake-river-estuary-shelf-ocean scales. SCHISM is stable even at high Courant
205 numbers and its code is fully parallelized, using the Message Passing Interface (MPI) standard.

206 Waves and sea surface elevation regional forecasts, combined with atmospheric and riverine
207 information, are then used to force local, high-resolution models that simulate water elevations

208 close to the coast and inside estuaries. Local-scale simulations are performed with SCHISM-
209 WWMII (Roland et al. 2012), which couples SCHISM with the spectral wave model WWM.
210 These two models share the same unstructured grid and its partition through the different MPI
211 application processes. The circulation model provides water elevations and velocities to the wave
212 model and receives the gradients of wave radiation stresses. This information is exchanged
213 through the memory (RAM), instead of files, which strongly contributes to the efficiency.

214 While the present modeling approach describes phase-averaged wave effects on the water levels
215 (wave setup), it neglects the effects at smaller time scales (wave uprush). This simplification is
216 required by the use of a phase-averaged wave model and often by the coarse grid resolution.
217 Inside estuaries, which are sheltered from the energetic sea waves, this simplification is usually
218 valid. For instance, the highest significant wave height measured and simulated inside the Tagus
219 estuary does not reach 1 m (Freire et al., 2009; Rusu et al., 2009) in spite of its large width. In
220 contrast, neglecting the wave uprush can severely underestimate inundation in the open coast.

221 WIFF's forecast system runs on a Linux operating system. Its core is composed by a set of
222 scripts, scheduled to run periodically, which prepare and launch each forecast simulation (Figure
223 2). The scripts interact with PostgreSQL databases to retrieve input data to force the models,
224 including river flows and atmospheric forecasts, and to store some results. Simulation
225 requirements include the results of the previous run, forecasts from global circulation and
226 atmospheric models and data from field sensors.

227 [Figure 2 near here]

228 In order to optimize the use of available computational resources, an optional execution
229 offloading process allows moving the execution away from the initiator resource. Each
230 simulation can thus be executed on the machine where the scripts were launched or sent to other
231 machines, often High Performance Computing (HPC) resources. To avoid having different code
232 paths depending on the kind of execution resources being used, the offload process is transparent
233 to the platform and completely model-agnostic. It uses the Secure Shell (SSH) services and Bash
234 scripting facilities to provide a secure, reliable, simple and flexible offloading process. Every day,
235 the system generates 48 hour forecasts of waves and sea levels.

236 **3. Demonstration case study**

237 ***3.1. General approach***

238 The major and deadliest storm surges usually occur in areas with wide continental shelves (Breilh
239 2014). With a continental shelf about 20-70 km wide, the Portuguese coast has thus been spared
240 from major catastrophes. Still, there are historical records of severe damages and casualties
241 associated to storm surges in the Portuguese coast (Freitas and Dias 2013), and in the Tagus
242 estuary in particular (Tavares et al. 2015). In 2014, the Hercules storm caused tens of millions
243 euros worth of damage along this coast. These events motivated the development of a forecast
244 system for extreme sea levels in the Portuguese coast.

245 The model setup is composed by three distinct applications (Figure 3): a regional scale wave
246 model; a regional scale tide and surge model; and a local scale coupled wave-circulation model.
247 The three applications are detailed below.

248 [Figure 3 near here]

249 ***3.2. Regional modeling: the North Atlantic and the Portuguese shelf***

250 Regional wave simulations are performed with one-way nesting. The first WW3 domain covers
251 the North Atlantic, from 0° to 70° N and from 0° to 80° W, with a 0.5° resolution (Figure 3). A
252 nested grid with a 0.05° resolution is then used in the Portuguese shelf. The time steps are set to
253 15 and 3 minutes for the coarse and fine grids, respectively. The wave spectrum is resolved with
254 24 directions and 25 frequency bins, following Dodet et al. (2010). The simulations are forced by
255 wind fields from GFS (Global Forecast System, www.ncdc.noaa.gov) with space and time
256 resolutions of 1.875° and 6 hours, respectively.

257 This deployment is operational since 2011, producing daily forecasts of 48 hours. Results are
258 compared automatically with online data from four wave buoys from the Portuguese
259 Hydrographic Institute and the Lisbon Harbor available along the Portuguese coast: Leixões,
260 Lisboa, Sines and Faro. In order to assess the accuracy of the forecasts, errors were computed at

261 these four stations for a period of 4 years, between 2011 and 2015 (Figure 4). The error metrics
262 selected were the root mean square error (RMSE), the RMSE normalized by the mean of the
263 observations (NRMSE) and the bias (Table 1). Results show the excellent behavior of the model
264 in the western Portuguese coast (Leixões, Lisboa and Sines), where the errors are similar to
265 hindcast models (e.g., Dodet et al. 2010; Rusu and Guedes Soares 2015). The model tends to
266 underestimate the significant wave heights (10 to 20 cm bias), but the error is small even for the
267 largest waves. Errors are larger in the southern coast (Faro buoy), possibly due to the inability of
268 the atmospheric model to adequately represent the wind fields in the Bay of Cadiz.

269 [Figure 4 near here] [Table 1 near here]

270 The differences between the forecasts made for the same day and for the following day are
271 negligible (Table 1), thus providing confidence in the use of the 48 hour forecasts. Also, since the
272 forcing wind fields are occasionally delivered with some delay, this small difference allows
273 WIFF to still generate reliable forecasts. In this situation, the WIFF forecast is forced by the most
274 recent atmospheric forecast, as long as it covers the whole forecast period (48h). This possibility
275 makes the system more resilient to failures.

276 Water levels due to tides and surges are simulated with SCHISM in depth-averaged barotropic
277 mode in a domain that covers a significant portion of the Northeast Atlantic (Fortunato et al.
278 2016a). The resolution is particularly fine in the Portuguese shelf, reaching 250 m. The model is
279 forced at the open boundaries by tides from the global tidal model FES2012 (Carrère et al. 2012)
280 and by the inverse barometer effect, to account for atmospheric pressure variations. Inside the
281 domain, the model is forced by the tidal potential, and forecasts of atmospheric pressure and wind
282 from NOAA's GFS.

283 The model has been running operationally since March 2015. Results from the forecasts between
284 March and December 2015 were compared with measurements at several Portuguese, Spanish
285 and French tide gauges (Table 2). RMS errors are of the order of 5-7 cm along the western
286 Iberian coast, and 11-13 cm in the Bay of Biscay. Fortunato et al. (2015) showed that the RMSE
287 for the present forecasts are about 10-35% smaller than those provided by a standard model in the
288 Portuguese coast (Maraldi et al. 2013). Time series of elevations and surges at the Cascais tide

289 gauge during a storm surge that hit the Portuguese coast in May 2016 show that the model is able
290 to reproduce elevations during energetic events (Figure 5a).

291 [Table 2 near here; Figure 5 near here]

292 **3.3. Local modeling: the Tagus estuary**

293 The SCHISM-WWMIII application covers a domain of about 120 km long, including a coastal
294 area with a radius of about 30 km (Figure 3). The local model is forced by results from the
295 regional wave and sea level models at the ocean boundary. Some areas particularly prone to
296 flooding, above the highest astronomical tide line (determined by Rilo et al. 2014), are included
297 in the model domain (Figure 6a). A digital terrain model was constructed using the most recent
298 bathymetric data from the Lisbon Harbor authority, LIDAR data of the coastal margins from the
299 Portuguese Environmental Agency, and high-resolution topography from the Direção Geral do
300 Território. The grid has about 80,000 nodes. The spatial resolution varies between 2 km at the
301 outer bay and typically 20-60 m close to the margins (Figure 6b). The time step is set to 30 s. The
302 friction coefficient in the estuary is defined based on the bed sediments (Guerreiro et al., 2015)
303 and on the land cover from Chen et al. (2015) on dry land. The river boundary is forced by
304 extrapolations of flow measurements (<http://www.snirh.pt>), which are automatically replaced by
305 climatology when unavailable. Atmospheric pressure and wind forecasts from the 9 km
306 implementation of the WRF model provided <http://www.windguru.cz> complete the model
307 forcings.

308 [Figure 6 near here]

309 The model was validated through four different tests. The first test verifies the ability of the
310 model to represent water levels variability throughout the estuary. Hindcast simulations were
311 performed, forced by tides and river flow. Results were compared with synthesized tides from 13
312 tidal gauges distributed throughout the estuary. Results show the excellent accuracy of the model,
313 with RMS errors of 4-16 cm (Table 3). These errors compare favorably with those previously
314 reported for the same dataset (Fortunato et al. 1999; Guerreiro et al. 2015). The second test

315 assesses the ability of the model to reproduce energetic events. The most severe warning
316 provided by the Tagus forecast system so far occurred on May 8, 2016, when over 30 cm of
317 water were predicted for Seixal. Inundations occurred as predicted, and traffic had to be
318 interrupted in the road that borders the estuary (Oliveira et al., 2016). Forecasts produced in May,
319 2016 are compared with tide gauge data at two stations (Figure 5b, c), showing the ability of the
320 model to reproduce storm surges. The third test verifies the ability of the model to reproduce
321 marginal inundation during an extreme event. The model was run for the period of the Xynthia
322 storm, between February 18 and March 4, 2010. The extent of the flooding that occurred during
323 those days in the Seixal old city center (Figure 6a) was determined through a post-event field
324 survey, by interviewing the local authorities and analyzing photographs taken during the event
325 (Freire et al., 2016). The extent of the flooding predicted by the model fully agrees with the field
326 survey data to within grid resolution accuracy: all the surveyed points are located within the layer
327 of partially wet elements (Figure 7). For the same event, the root mean square error of the
328 elevations at the Cascais tide gauge was 7.5 cm. Finally, the fourth test verifies the ability of the
329 model to produce accurate results away from the ocean boundary in forecast mode by comparing
330 model results with data obtained with a Level Troll 700 tidal gauge installed in the Seixal Bay
331 (Figure 8a) between March 20 and 31, 2015. The model accuracy is similar to the one obtained in
332 hindcast mode, with a RMS error of 13 cm (Figure 8b). Together, the four tests show that the
333 model accurately forecasts the flooding associated to extreme events in the Tagus estuary.

334 [Figures 7, 8 near here] [Table 3 near here]

335 ***3.4. WIFF deployment for the Tagus estuary***

336 The WIFF deployment for the Tagus estuary is organized along four main components: early-
337 warning, flood forecast, forcings and risk analysis (Figure 9a). The first component provides
338 information on the vulnerable areas that may be flooded in the next 48 hours. The Seixal
339 Municipality waterfront, which is flooded on a yearly basis, was chosen as a local-scale case for
340 the warning component implementation (Freire et al., 2016). At selected critical points along the
341 margins, the total water depth is evaluated every 15 minutes. Warnings of different levels of

342 inundation severity are provided when predefined thresholds are exceeded (Figure 9b) and an
343 early-warning bulletin is automatically generated and sent by email to the civil protection agents.
344 The flood forecast component uses layer maps, sourced from shapefile format files, and makes
345 them available through geo-referenced maps (Figure 9c). These maps provide zoom and pan
346 capabilities, as well as the ability to switch layers on and off and superimpose them. The
347 forecasts are grouped by days and made available at each hour. This component also offers the
348 possibility to visualize monitoring data, compare them to the model results and download this
349 information in CSV format (Figure 9d). The forcings component provides access to the public
350 site with the regional forecasts. Model results can be accessed as animations or as time series, and
351 data/model comparisons can be performed. Finally, the risk analysis component provides access
352 to both hazard and vulnerability maps.

353 [Figure 9 near here]

354 Since March 2016 the WIFF deployment for the Tagus estuary has been used by the Seixal
355 Municipal Service for Civil Protection as a support tool for flood emergency management. So far,
356 the flood warning alerts that occurred consisted mostly in the lowest warning level (yellow,
357 corresponding to less than 0.2 m of water height). These warnings have been validated by in situ
358 observations and the acquired experience on past flood events by the civil protection services.
359 The early-warning bulletins have been particularly useful as a way to disseminate the relevant
360 information for planning the emergency response through the several civil protection agents (e.g.,
361 fire brigades, police). However, a detailed evaluation of the impact of WIFF as a decision-making
362 supporting tool for the emergency managers requires a longer operation of the system,
363 particularly during extreme water level events.

364 **4. Summary, discussion and outlook**

365 A new computational forecast framework for flood risk management was developed and
366 implemented in the Portuguese coast. The IT system is accurate, robust and agile and can be
367 extended to other estuaries and coastal zones and to other emergency concerns. The regional-

368 scale results are publicly available, while the local-scale forecasts are only available to the coastal
369 and emergency authorities, tailoring details and confidentiality of information to comply with the
370 user requirements. By supporting the forecasts on high-resolution models that solve the adequate
371 physical processes and their interactions, and making the results available at a friendly, multi-
372 device interface, the proposed framework contributes to an enhanced support to coastal
373 managers.

374 Forecast frameworks such as the one introduced herein can thus play a major role in optimizing
375 the response of the authorities to extreme events, thereby avoiding or mitigating the effects of
376 major disasters. The development of these systems is therefore expected to continue in the near
377 future. However, several challenges remain to be addressed.

378 It is unclear at this point whether and how the full forecasts should be disclosed to the public, and
379 there are strong arguments on both sides (Morrow et al. 2015). Clearly, a better informed public
380 can avoid irrational decisions, both in the short-term (e.g., going to the sea-side during severe
381 maritime conditions) and in the long-term (e.g., purchasing property in areas at risk). However,
382 many coastal managers strongly oppose the open release of this type of information to the public,
383 arguing that model results can be misread by the public, causing unjustified panic or false
384 assurance. The approach followed in WIFF is to disclose the coarse-resolution results from the
385 regional models to the public and make the results from the local model available to the proper
386 authorities only. The decision on informing the public will be made by these authorities based on
387 information from different sources. The adequate approach to disclose complex information such
388 as those provided by the models used herein to the general public is also a challenge as it requires
389 a detailed usability and public acceptance analysis.

390 Unveiling the forecasts to the public must take into account the uncertainty associated to the
391 predictions. Indeed, in spite of the excellent accuracy of the models shown above, significant
392 sources of errors remain. While the water elevation can be determined with errors of the order of
393 0.01-1 m (e.g., Bertin et al. 2012; Kerr et al. 2013), the uncertainty in the determination of the
394 position of the water line is significantly higher. This uncertainty has several sources, including
395 the model's horizontal resolution, and its inability to resolve short-scale features, common in

396 urban areas; the low topographic gradients, which amplify vertical errors in the water elevation;
397 outdated or inaccurate digital terrain models; neglecting water infiltration and sewage systems.
398 Yet, the position of the water line is one of the key information required by end-users. Estimating
399 this uncertainty and conveying it to the end-users is therefore a clear requirement for the forecast
400 systems, and sophisticated approaches based on ensemble simulations are now starting to be
401 followed (Höllt et al. 2015). In the Portuguese shelf, the sea surface variability is strongly
402 dominated by tides, which are easier to reproduce accurately than storm surges. Hence, the
403 uncertainty is lower than in areas of the world where storm surges can reach several meters. The
404 system described herein deals with the communication of uncertainty in two simple ways. First,
405 real-time data/model comparisons are an integral part of the system (Figure 9d). The user can
406 therefore obtain daily estimates of the errors. Secondly, the land-water interface is shown as a
407 strip, rather than a line. The strip is composed by the elements that have both wet and dry nodes
408 (Figure 7). While these details of the forecast system do not convey all the uncertainty associated
409 with the predictions, they help showing the end-user that models are not reality.

410 Forecast systems should provide information on a continuous basis. They are therefore totally
411 autonomous, and should be able to run without human intervention. However, they can fail for
412 several reasons, including power failures, internet communication failures and unavailability of
413 the driving atmospheric forecasts and other inputs. Not only can these failures have an impact on
414 the end-users, but they can also entail significant maintenance costs in terms of human resources.
415 The reliability of the system should thus be maximized. In WIFF, all forecasts run redundantly on
416 two different computers, with a few hours' delay, and most forcings have alternative sources
417 when the primary source fails. Further robustness can be obtained by resorting to cloud
418 computing services (Rogeiro et al. 2015), which can also be a way to progress in porting forecast
419 systems to the hands of the coastal managers.

420 This system will continue to be enhanced through the improvement of the models, the inclusion
421 of new datasets and local models, the extension of the forecast periods, the optimization of the
422 codes and the development of additional services provided by the interface. Risk criteria are also
423 being developed, in order to provide automatic alerts to the authorities.

424 **Acknowledgements**

425 This work was partially funded by the Fundação para a Ciência e a Tecnologia, through project
426 MOLINES (PTDC/AAG-MAA/2811/2012) and three grants (M. Rodrigues:
427 SFRH/BPD/87512/2012; A. Azevedo: SFRH/BPD/73089/2010; G. Jesus:
428 SFRH/BD/82489/2011) and the Portuguese National Distributed Computing Infrastructure
429 (INCD). The authors thank Dr. Xavier Bertin for useful discussions, Prof. Margarida Liberato for
430 providing the atmospheric forcings for the 2010 simulation, and the various institutions that
431 provided bathymetric, topographic, wave and sea surface elevation data and atmospheric model
432 forecasts. They also thank the authors of SCHISM, WWM and WW3 for making their models
433 available.

434 **References**

- 435 Anselmi-Molina CM, Canals M, Morell J, Gonzalez J, Capella J, Mercado A. 2012. Development
436 of an operational nearshore wave forecast system for Puerto Rico and the U.S. Virgin
437 Islands. *Journal of Coastal Research*, 28/5: pp. 1049 – 1056
- 438 Bajo M, Umgiesser G. 2010. Storm surge forecast through a combination of dynamic and neural
439 network models. *Ocean Modelling*, 33: 1-9. DOI:10.1016/j.ocemod.2009.12.007
- 440 Baptista AM. 2006. CORIE: the first decade of a coastal-margin collaborative observatory.
441 *Oceans'06*, MTS/ IEEE, Boston, MA.
- 442 Baptista AM, Seaton C, Wilkin M, Riseman S, Needoba JA, Maier D, Turner PJ, Karna T, Lopez
443 JE, Herfort L, Megler VM, McNeil C, Crump BC, Peterson TD, Spitz Y, Simon HM. 2015.
444 Infrastructure for collaborative science and societal applications in the Columbia River
445 estuary. *Frontiers of Earth Science*. 9(4):659-682.
- 446 Bertin X, Bruneau N, Breilh J-F, Fortunato AB, Karpytchev M. 2012. Importance of wave age
447 and resonance in storm surges: The case Xynthia, Bay of Biscay. *Ocean Modelling* 42/1: 16-
448 30. DOI: 10.1016/j.ocemod.2011.11.001
- 449 Blain CA, Westerink JJ, Luettich Jr. RA 1994. The influence of domain size on the response
450 characteristics of a hurricane storm surge model, *Journal of Geophysical Research*,
451 99(C9):18,467-18,479. DOI: 10.1029/94JC01348.
- 452 Breilh J-F. 2014. *Les surcotes et les submersions marines dans la partie centrale du Golfe de*
453 *Gascogne : les enseignements de la tempête Xynthia*, Ph.D. Thesis, Université de la
454 Rochelle, 225 pp.
- 455 Carrère L, Lyard F, Cancet M, Guillot A, Roblou L. 2012. FES2012: A new global tidal model
456 taking taking advantage of nearly 20 years of altimetry, *Proceedings of meeting "20 Years of*
457 *Altimetry"*.

- 458 Castelle B, Marieu V, Bujan S, Splinter KD, Robinet A, Senechal N, Ferreira S. 2015. Impact of
459 the winter 2013-2014 series of severe Western Europe storms on a double-barred sandy
460 coast: Beach and dune erosion and megacusp embayments, *Geomorphology*, 238: 135-148.
461 DOI: 10.1016/j.geomorph.2015.03.006.
- 462 Chandrasekar K, Pathridge M, Wijeratne S, Mattocks C, Plale B. 2012. Middleware alternatives
463 for storm surge predictions in Windows Azure, in “*Proceedings of the 3rd workshop on*
464 *Scientific Cloud Computing*”, 3-12.
- 465 Chen J, Chen J, Liao A, Cao X, Chen L, Chen X, He C, Peng S, Lu M, Zhang W, Tong X, Mills
466 J. 2015. Global land cover mapping at 30 m resolution: A POK-based operational approach,
467 ISPRS Journal of Photogrammetry and Remote Sensing: DOI:
468 10.1016/j.isprsjprs.2014.09.002.
- 469 David LM, Oliveira A, Rodrigues M, Jesus G, Póvoa P, David C, Costa R, Fortunato AB, Menaia
470 J, Frazão M, Matos RS. 2013. Development of an integrated system for early warning of
471 recreational waters contamination. In “*Proceedings of the 8th Int. Conf. on Sustainable*
472 *Techniques and Strategies in Urban Water Management (Novatech’2013)*”, Lyon, France,
473 CD-ROM, 10 p, 2013.
- 474 Daniel P, Josse P, Dandin P, Lefevre JM, Lery G, Cabioc’h F, Gouriou V. 2004. Forecasting the
475 Prestige oil spills, in “*Proceedings of the Interspill 2004*”.
- 476 Dietrich JC, Zijlema M, Westerink JJ, Holthuijsen LH, Dawson C, Luetlich RA Jr., Jensen RE,
477 Smith JM, Stelling GS, Stone GW. 2011. Modeling hurricane waves and storm surge using
478 integrally-coupled, scalable computations. *Coastal Engineering*, 58/1: 45-65. DOI:
479 10.1016/j.coastaleng.2010.08.001.
- 480 Dodet G, Bertin X, Taborda R. 2010. Wave climate variability in the North-East Atlantic Ocean
481 over the last six decades. *Ocean Modelling*, 31/3-4: 120-131. DOI:
482 10.1016/j.ocemod.2009.10.010.
- 483 Dresback KM, Fleming JG, Blanton BO, Kaiser C, Gourley JJ, Tromble EM, Luetlich, Jr. RA,
484 Kolar RL, Hong Y, van Cooten S, et al. 2013. Skill Assessment of a Real-Time Forecast
485 System Utilizing a Coupled Hydrologic and Coastal Hydrodynamic Modeling During
486 Hurricane Irene (2011). *Continental Shelf Research*, 71: 78-94. DOI:
487 10.1016/j.csr.2013.10.007.
- 488 Fortunato AB, Oliveira A, Baptista AM. (1999). On the effect of tidal flats on the hydrodynamics
489 of the Tagus estuary. *Oceanologica Acta*, 22/1: 31-44. DOI:10.1016/s0399-1784(99)80030-
490 9.
- 491 Fortunato AB, Tavares da Costa R, Rogeiro J, Gomes JL, Oliveira A, Li K, Freire P, Rilo A,
492 Mendes A, Rodrigues M. 2015. Desenvolvimento de um sistema operacional de previsão de
493 temporais na costa portuguesa, *VIII Congresso sobre Planeamento e Gestão das Zonas*
494 *Costeiras dos Países de Expressão Portuguesa*, 15 pp (in Portuguese).

- 495 Fortunato AB, Li K, Bertin X, Rodrigues M, Miguez BM. 2016a. Determination of extreme sea
496 levels along the Iberian Atlantic coast, *Ocean Engineering*, 111/1: 471-482.
- 497 Fortunato AB, Freire P, Bertin X, Rodrigues M, Liberato MLR, Ferreira J 2016b. Inundação das
498 margens do estuário do Tejo: o caso da tempestade de fevereiro de 1941, *Actas das 4as*
499 *Jornadas de Engenharia Hidrográfica*, Instituto Hidrográfico, 143-146 (in Portuguese).
- 500 Freire, P., Ferreira, Ó., Taborda, R., Oliveira, F.S.B.F., Carrasco, A.R., Silva, A., Vargas, C.,
501 Capitão, R., Fortes, C.J., Coli, A.B., Santos, J.A. (2009). Morphodynamics of fetch-limited
502 beaches in contrasting environments, *Journal of Coastal Research*, Special Issue 56, 183-
503 187.
- 504 Freire, P., Tavares, A., Sá, L., Oliveira, A., Fortunato, A.B., Santos, P.P., Rilo, A., Gomes, J.L.,
505 Rogeiro, J., Pablo, R., Pinto, P.J. (2016). A local scale approach to estuarine flood risk
506 management, *Natural Hazards*, doi:10.1007/s11069-016-2510-y
- 507 Freitas JG, Dias JA. 2013. 1941 windstorm effects on the Portuguese Coast. What lessons for the
508 future? *Journal of Coastal Research*, Special Issue 65: 714-719. DOI: 10.2112/SI65-121.
- 509 Gallien TW, Barnard PL, van Ormondt M, Foxgrover AC, Sanders BF. 2013. A parcel-scale
510 coastal flood forecasting prototype for a Southern California urbanized embayment. *Journal*
511 *of Coastal Research*, 29/3: 642-656. DOI: 10.2112/jcoastres-d-12-00114.1.
- 512 Gomes JL, Jesus G, Rogeiro J, Oliveira A, Costa R, Fortunato AB. 2015.
513 Molines – towards a responsive Web platform for flood forecasting and risk
514 mitigation. *Proceedings of the Federated Conference on Computer Science and*
515 *Information Systems* pp. 1171–1176 ACSIS, Vol. 5 DOI: 10.15439/2015F265.
- 516 Guerreiro M, Fortunato AB, Freire P, Rilo A, Taborda R, Freitas MC, Andrade C, Silva T,
517 Rodrigues M, Bertin X, Azevedo A. 2015. Evolution of the hydrodynamics of the Tagus
518 estuary (Portugal) in the 21st century. *Revista de Gestão Costeira Integrada*, 15/1: 65-80.
519 DOI: 10.5894/rgci515
- 520 Herold S, Sawada M, Wellar B. 2005. Integrating geographic information systems, spatial
521 databases and the internet: a framework for disaster management. *Proceedings of the 98th*
522 *Annual Canadian Institute of Geomatics Conference*, pp. 13-15.
- 523 Höllt T, Altaf MU, Mandli KT, Hadwiger M, Dawson CN, Hoteit I. 2015. Visualizing
524 uncertainties in a storm surge ensemble data assimilation and forecasting system. *Natural*
525 *Hazards*, 77/1: 317-336. DOI: 10.1007/s11069-015-1596-y
- 526 Jesus G, Gomes J, Ribeiro NA, Oliveira A. 2012. Custom deployment of a Nowcast-forecast
527 information system in coastal regions, *Geomundus* 2012.
- 528 Kerr PC, Donahue AS, Westerink JJ, Luettich Jr., RA, Zheng LY, Weisberg RH, Huang Y, Wang
529 HV, Teng Y, Forrest DR, Roland A, et al. 2013. US IOOS coastal and ocean modeling
530 testbed: Inter-model evaluation of tides, waves, and hurricane surge in the Gulf of Mexico.
531 *Journal of Geophysical Research-Oceans*, 118/10: 5129-5172. DOI: 10.1002/jgrc.20376.

- 532 Kyng M, Nielsen ET, Kristensen M. 2006. Challenges in designing interactive systems for
533 emergency response. In *Proceedings of the 6th ACM Conference on Designing interactive*
534 *Systems*, ACM Press, pp. 301-310.
- 535 Kulkarni AT, Mohanty J, Eldho TI, Rao EP, Mohan BK. 2014. A web GIS based integrated flood
536 assessment modeling tool for coastal urban watersheds. *Computers & Geosciences* 64: 7-14.
537 DOI:10.1016/J.CAGEO.2013.11.002
- 538 Liberato MLR, Pinto JG, Trigo RM, Ludwig P, Ordóñez P, Yuen D, Trigo IF. 2013. Explosive
539 development of winter storm Xynthia over the subtropical North Atlantic Ocean. *Natural*
540 *Hazards and Earth System Science*, 13, 2239–2251. DOI: 10.5194/nhess-13-2239-2013
- 541 Maraldi C, Chanut J, Levier B, Ayoub N, De Mey P, Reffray G, Lyard F, Cailleau S, Drévilion
542 M, Fanjul EA, et al. 2013. NEMO on the shelf: assessment of the Iberia–Biscay–Ireland
543 Configuration, *Ocean Science*, 9: 745–771. DOI: 10.5194/os-9-745-2013
- 544 Morrow BH, Lazo JK, Rhome J, Feyen J. 2015. Improving storm surge risk communication.
545 Stakeholder perspectives. *Bulletin of the American Meteorological Society*, 96/1: 35-48.
546 DOI: 10.1175/bams-d-13-00197.1
- 547 Oliveira A, Jesus G, Gomes JL, Rogeiro J, Azevedo A, Rodrigues M, Fortunato AB, Dias JM,
548 Tomás LM, Vaz L, et al. 2014. An interactive WebGIS observatory platform for enhanced
549 support of integrated coastal management. *Journal of Coastal Research*, Special Issue 70:
550 507 - 512. DOI: 10.2112/SI70-086.1.
- 551 Oliveira A, Rogeiro J, Gomes JL, Pinto P, Fortunato AB, Freire P, Costa RT, Sá L, Pablo R,
552 Mendes A 2016. Plataforma integrada WebSIG para apoio à gestão da emergência em
553 eventos de inundação em estuários, *Actas das 4as Jornadas de Engenharia Hidrográfica*,
554 Instituto Hidrográfico, 121-124 (in Portuguese).
- 555 Ramakrishnan L, Blanton BO, Lander H, Luettich RA, Reed, DA, Thorpe SR. 2006. Real-time
556 storm surge ensemble modeling in a grid environment. In: *Second International Workshop*
557 *on Grid Computing Environments* (GCE).
- 558 Rilo A, Freire P, Mendes RN, Ceia R, Catalão J, Taborda R, Melo R, Caçador MI, Freitas MC,
559 Fortunato AB, Alves E. 2014. Methodological framework for the definition and demarcation
560 of the highest astronomical tide line in estuaries: the case of Tagus Estuary (Portugal),
561 *Revista de Gestão Costeira Integrada*, 14/1: 95-107 (in Portuguese). DOI:10.5894/rgci450
- 562 Rogeiro J, Azevedo A, Rodrigues M, Oliveira A. 2015. Running high resolution coastal
563 forecasts: moving from grid to cloud resources, in J. Kruis, Y. Tsompanakis, B.H.V.
564 Topping, (Editors), *Proceedings of the Fifteenth International Conference on Civil,*
565 *Structural and Environmental Engineering Computing*, Civil-Comp Press, Stirlingshire, UK,
566 Paper 218, 2015. doi:10.4203/ccp.108.218
- 567 Roland A, Zhang YJ, Wang HV, Meng Y, Teng Y-C, Maderich V, Brovchenko I, Dutour-Sikiric
568 M, Zanke U. 2012. A fully coupled 3D wave-current interaction model on unstructured grids.
569 *Journal of Geophysical Research*, 117, C00J33. DOI: 10.1029/2012JC007952.

- 570 Rusu, L., Bernardino, M., Guedes Soares, C. (2009). Influence of wind resolution on the
571 prediction of waves generated in an estuary, *Journal of Coastal Research*, Special Issue 56:
572 1419-1423.
- 573 Rusu L, Guedes Soares C. 2015. Impact of assimilating altimeter data on wave predictions in the
574 western Iberian coast, *Ocean Modelling*, 96: 126-135 DOI: 10.1016/j.ocemod.2015.07.016
- 575 Tavares AO, Santos PP, Freire P, Fortunato AB, Rilo A, Sá L. 2015. Flooding hazard in the
576 Tagus estuarine area: the challenge of scale in vulnerability assessments. *Environmental*
577 *Science & Policy*, 51: 238-255. DOI: 10.1016/j.envsci.2015.04.010.
- 578 Tolman HL. 2009. User manual and system documentation of WAVEWATCH III, version 3.14.
579 NOAA/NWS/NCEP/MMAB Technical Note 276, 194 p.
- 580 Wernera M, Schellekens J, Gijbers P, van Dijkstra M, van den Akker O, Heynert K. 2013. The
581 Delft-FEWS flow forecasting system. *Environmental Modelling & Software*, 40: 65-77.
582 DOI: 10.1016/j.envsoft.2012.07.010.
- 583 Zhang K, Li Y, Liu H, Rhome J, Forbes C. 2013. Transition of the Coastal and Estuarine Storm
584 Tide Model to an operational storm surge forecast model: a case study of the Florida coast.
585 *Weather and Forecasting*, 28/4: 1019-1037. DOI: 10.1175/waf-d-12-00076.1.
- 586 Zhang Y, Baptista AM. 2008. SELFE: A semi-implicit Eulerian-Lagrangian finite-element
587 model for cross-scale ocean circulation. *Ocean Modeling*, 21(3-4), 71-96. DOI:
588 10.1016/j.ocemod.2007.11.005.
- 589 Zhang YJ, Ye F, Stanev EV, Grashorn S. 2016. Seamless cross-scale modeling with SCHISM,
590 *Ocean Modelling*, 102: 64-81.

591 **Tables**

592 **Table 1. Validation of the wave forecasts between 2011 and 2015 at four wave buoys along**
 593 **the Portuguese coast. Values between brackets refer to forecasts made for the following**
 594 **day.**

Error measure	Leixões	Lisboa	Sines	Faro
RMSE (cm)	32 (33)	30 (30)	34 (34)	44 (44)
NRMSE (%)	17 (18)	27 (28)	22 (23)	48 (49)
Bias (cm)	16 (16)	23 (23)	8 (9)	-19 (-20)
Longitude	-9.10	-9.4	-8.95	-7.90
Latitude	41.20	38.6	37.90	36.90
Depth (m)	83	73	97	107

595

596

597 **Table 2. Validation of the regional tide and surge model: RMSE obtained for the forecasts**
 598 **from March to December 2015. Data were retrieved from <http://www.emodnet.eu>. The**
 599 **mean sea level was removed from the time series before the evaluation of the error due to**
 600 **doubts on the reference level at some stations.**

Station	RMSE (cm)
Las Palmas	6.7
Huelva	6.6
Sines	5.2
Peniche	6.2
Nazaré	6.3
Leixões	7.0
Vigo	6.6
La Coruña	12.8
Gijón	11.6
Santander	11.7
Bilbao	12.5
Port Bloc	11.9
Socoa	13.6

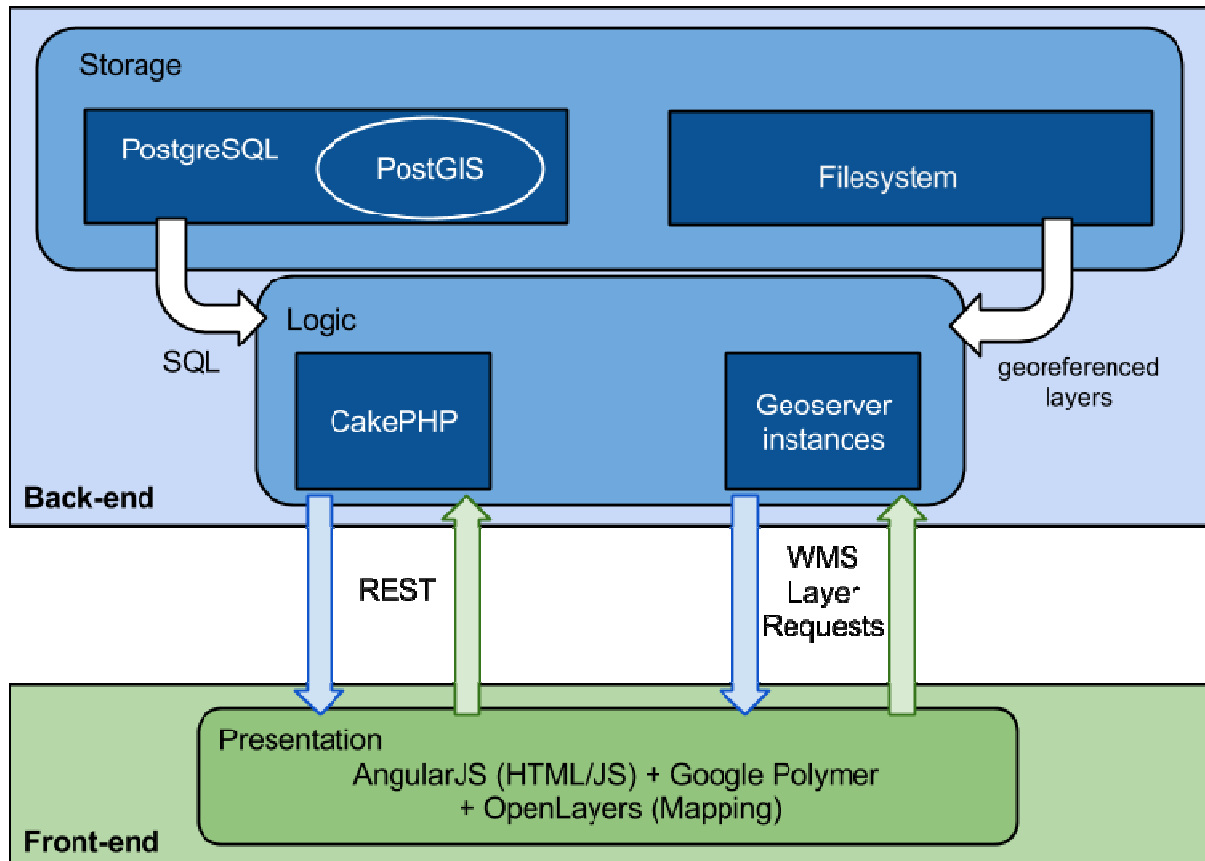
601

602 **Table 3. Validation of the Tagus model in hindcast mode: RMSE at 13 tidal stations. The**
603 **position of the stations is indicated in Figure 3.**

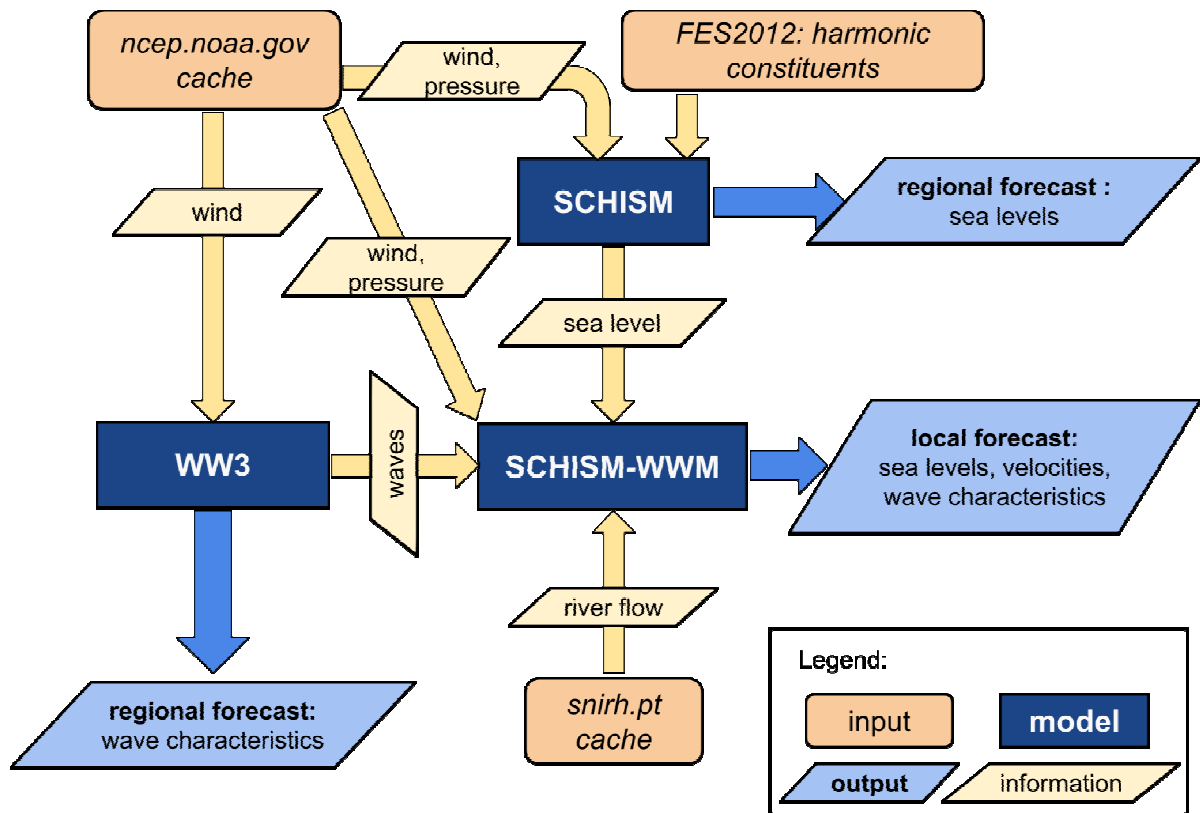
Station	RMSE (cm)
Cascais	4.6
P. Arcos	3.7
Trafaria	5.3
Lisboa	5.9
Pedrouços	4.1
Cacilhas	5.3
Seixal	6.4
Montijo	6.5
C. Ruivo	8.5
Alcochete	12.0
Sta. Iria	15.6
Pta. Erva	15.7
Vila Franca	12.0

604

605 **Figure captions**

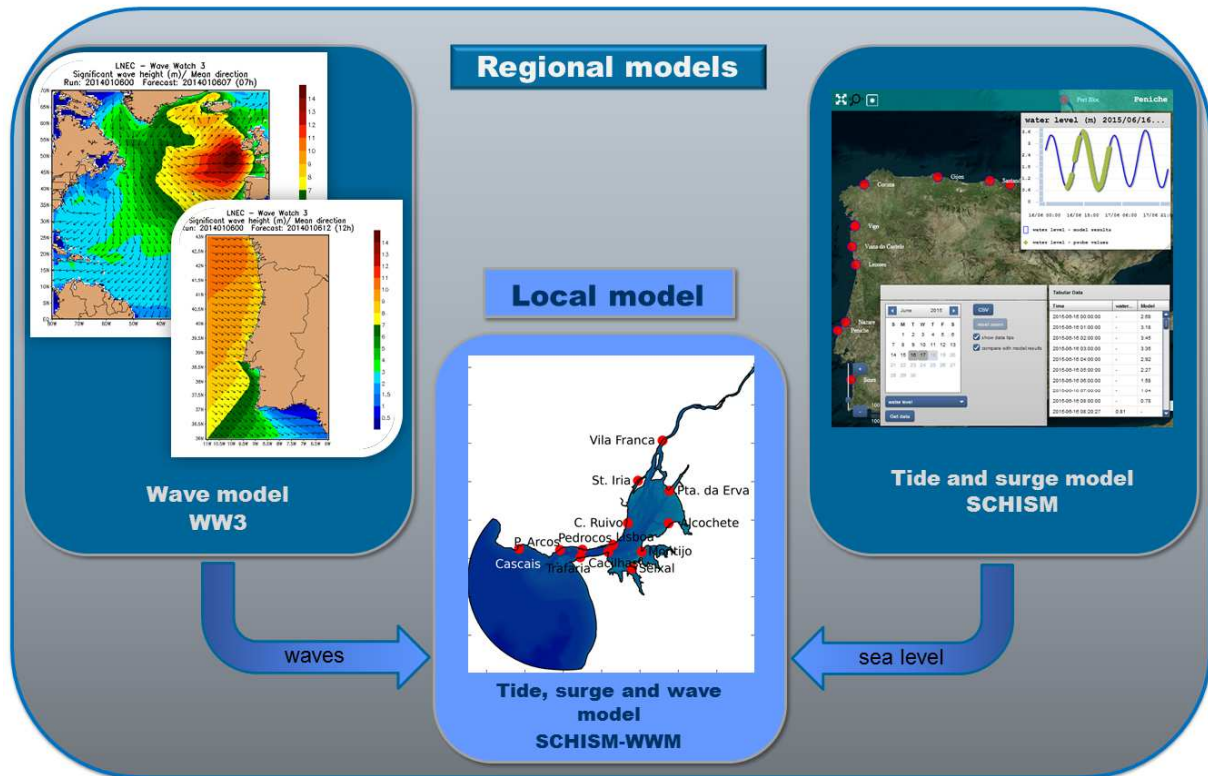


606
607 **Figure 1. Information flow between the back-end and the front-end.**

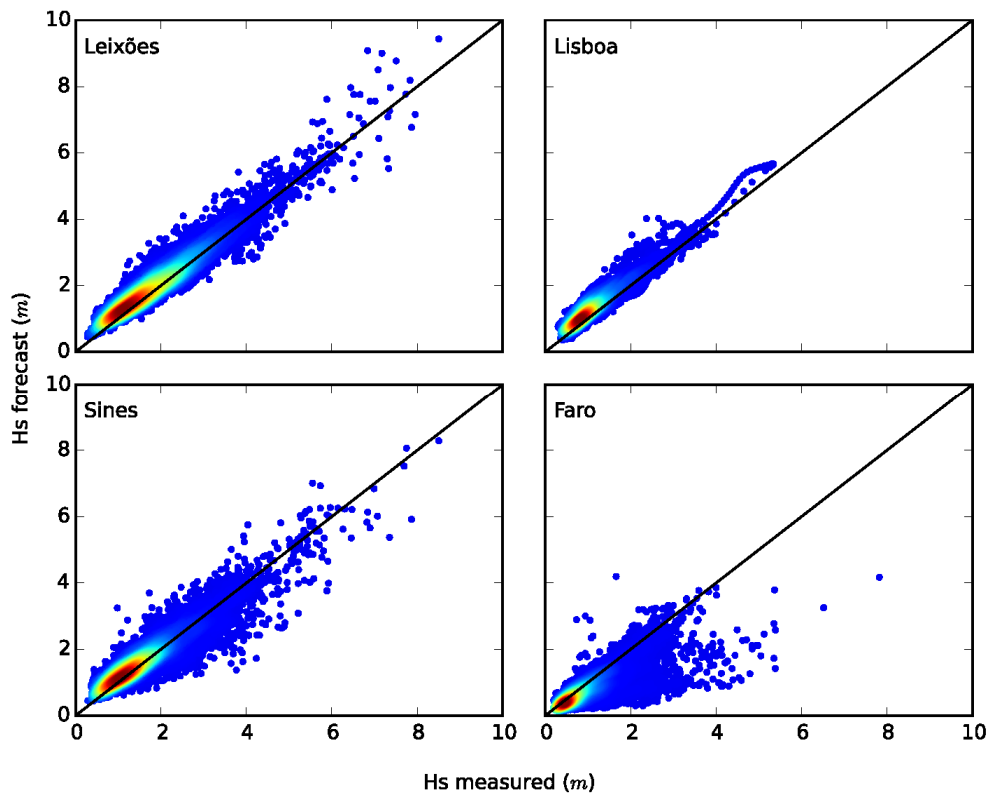


608

609 **Figure 2. Procedure workflow for the wave / current forecasts in the Tagus estuary.**

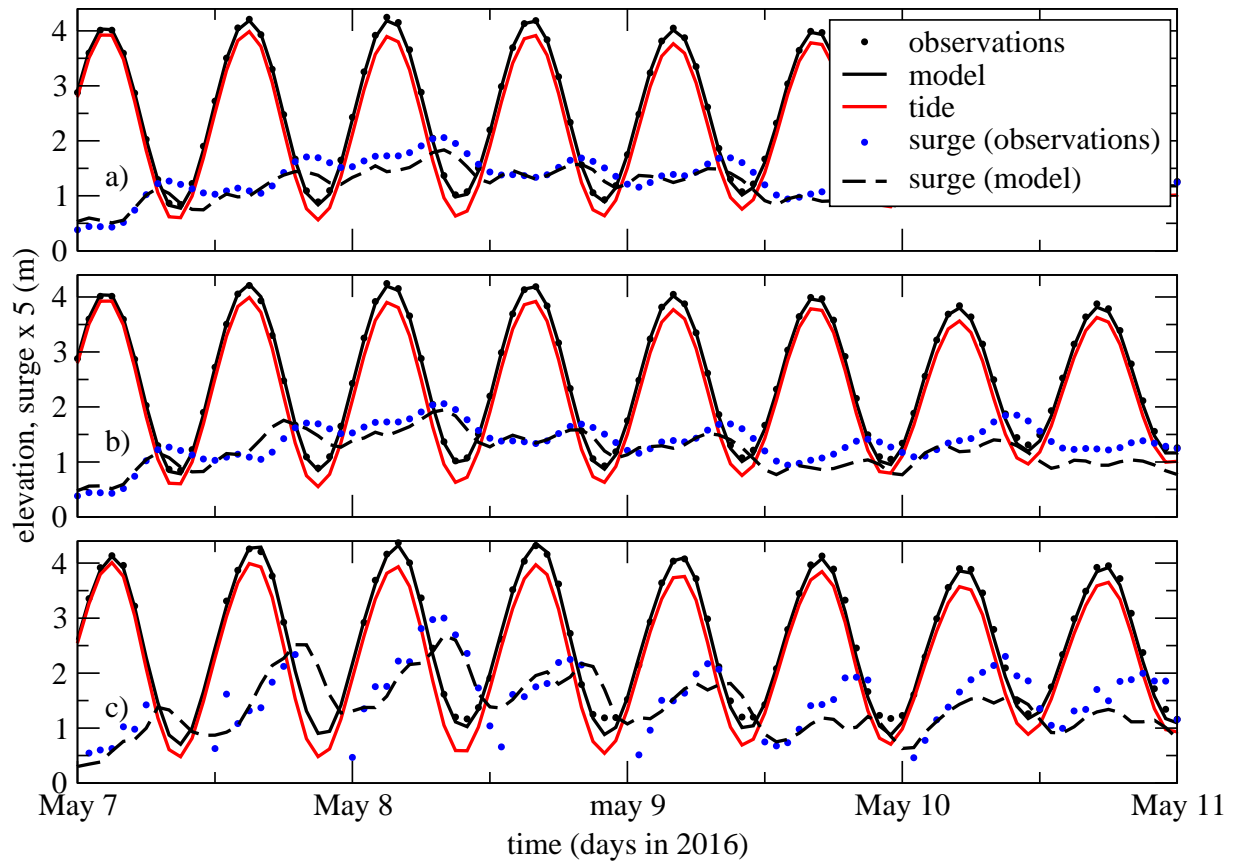


610
 611 **Figure 3. Generic modeling scheme. The figures of the wave model show the significant**
 612 **wave heights forecasts in early January 2014, during the Hercules storm. The figure of the**
 613 **regional tide and surge model shows an aspect of the public interface, with the model/data**
 614 **comparison (<http://ariel.lnec.pt>). The figure of the Tagus estuary shows the bathymetry, the**
 615 **model domain and the tidal stations used for validation in hindcast mode.**



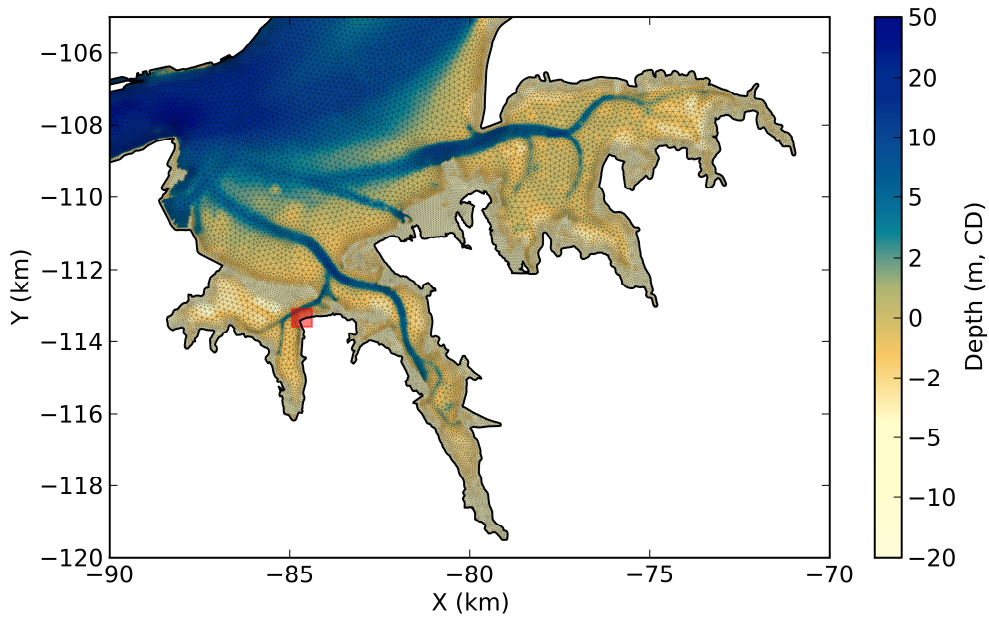
616

617 **Figure 4. Validation of the wave forecasts between 2011 and 2015 at four wave buoys along**
 618 **the Portuguese coast: comparison between Hs estimated from measurements and forecast**
 619 **results made on the same day.**

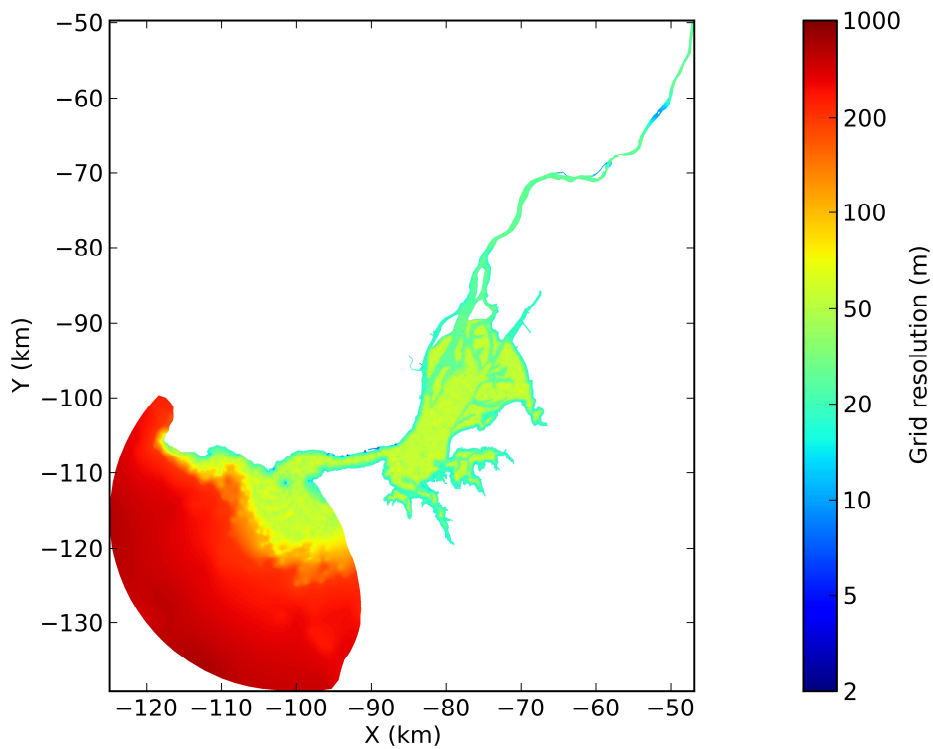


620

621 **Figure 5. Validation of the tide surge models during a storm surge event in May, 2016: a)**
 622 **data and results from the regional model at Cascais; b) data and results from the Tagus**
 623 **model at Cascais; c) data and results from the Tagus model at Pedrouços. All surges were**
 624 **multiplied by 5 for clarity. Tides were synthesized from model results.**

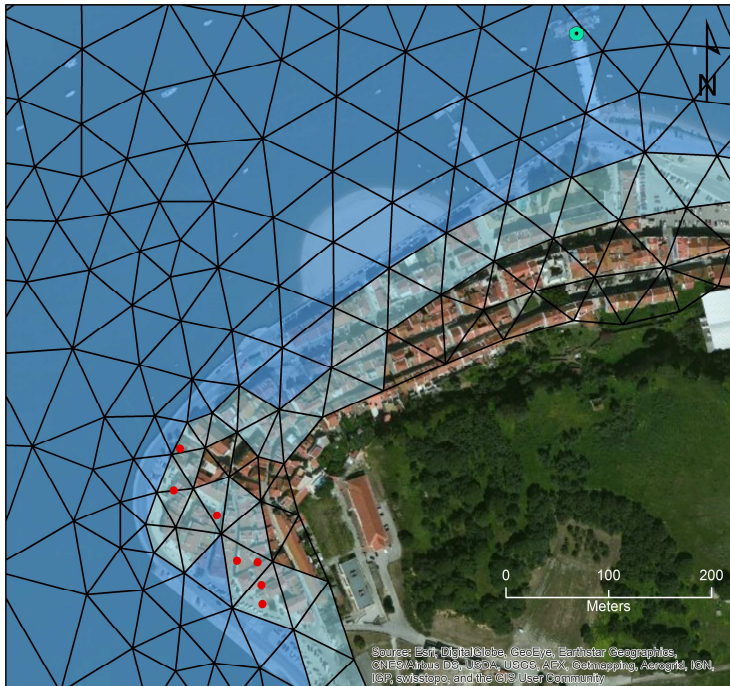


625



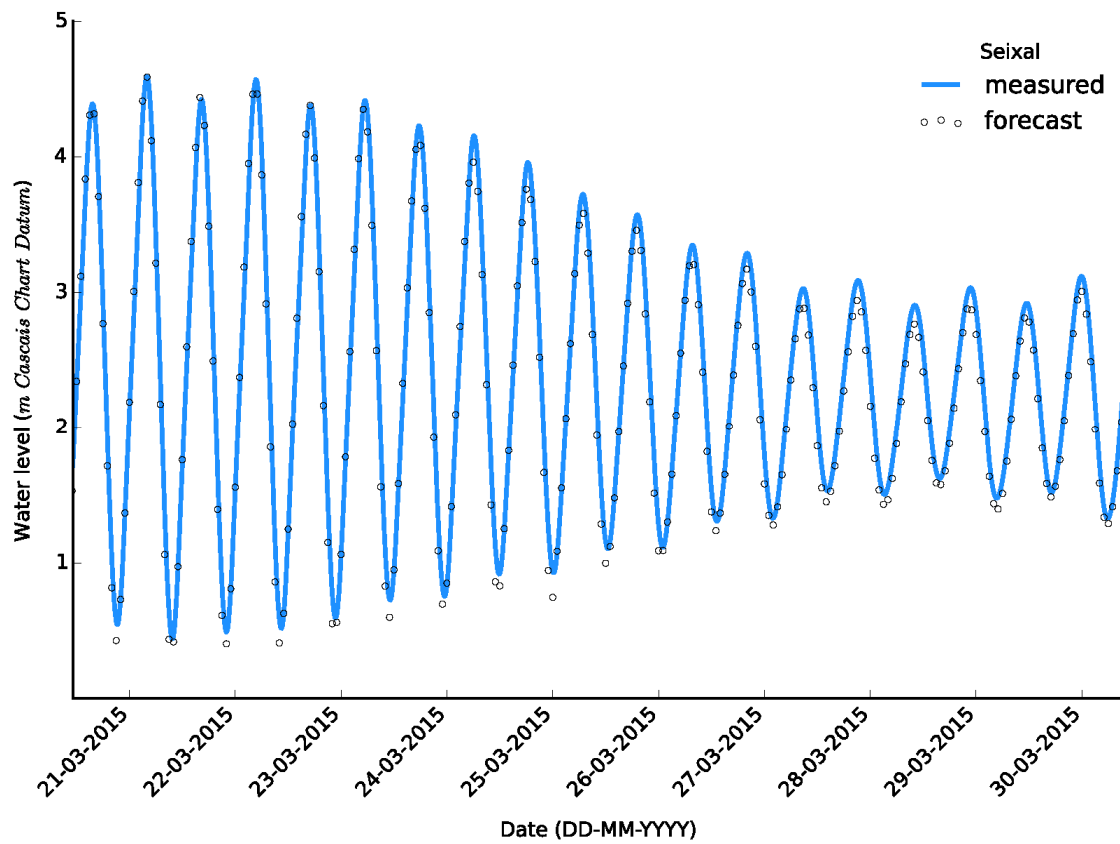
626

627 **Figure 6. Tagus model grid: a) detail of the grid and bathymetry in the Seixal area; b) grid**
 628 **resolution, defined as the equivalent element diameter. The red square in a) indicates the**
 629 **area shown in Figure 7.**




630

631 **Figure 7. Validation of the Tagus model for an extreme event (Xynthia storm, February**
 632 **2010). The location of this area is shown in Figure 6a). The red circles indicate the surveyed**
 633 **extent of the flooding in the city of Seixal. The wet elements (elements with three wet nodes)**
 634 **are indicated in dark blue, and the partially wet elements (elements with one or two wet**
 635 **nodes) are shown in light blue. The green circle indicates the location of the temporary**
 636 **monitoring station at Seixal (X= -84489.407 m; Y= -113102.754 m, ETRS89 TM-06).**




637

638 **Figure 8. Validation of the Tagus model in forecast mode: comparison between**
 639 **observations and model results at the Seixal temporary station (Figure 7). The RMS error**
 640 **is 13 cm.**


 **OLINES**
Sistema de Alertas

Alertas para o dia de hoje (Previsão de 2016-01-07 00:00:00 a 2016-01-09 00:00:00)

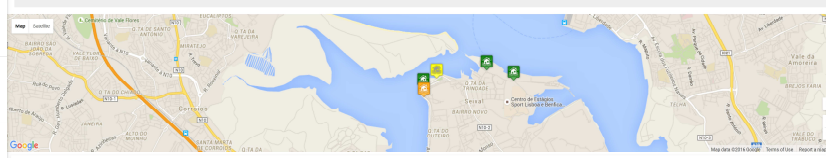
Zona	Baixo	Medio	Risco
Corroios	2	0	0
Amora	3	0	0
Seixal, Arrentela e Paio Pires	3	1	1



641

 **OLINES**
Sistema de Alertas

Freguesia Seixal, Arrentela e Paio Pires Previsão de 2016-01-07 00:00:00 a 2016-01-09 00:00:00



Local: Curva Mundet
Risco: Medio
(Previsão de 2016-01-07 00:00:00 a 2016-01-09 00:00:00)

0h	1h	2h	3h	4h	5h	6h	7h	8h	9h	10h	11h	12h	13h	14h	15h	16h	17h	18h	19h	20h	21h	22h	23h
0h	1h	2h	3h	4h	5h	6h	7h	8h	9h	10h	11h	12h	13h	14h	15h	16h	17h	18h	19h	20h	21h	22h	23h

BOLETIM DO ALERTA

Local: Igreja Seixal
Risco: Sem risco
(Previsão de 2016-01-07 00:00:00 a 2016-01-09 00:00:00)

0h	1h	2h	3h	4h	5h	6h	7h	8h	9h	10h	11h	12h	13h	14h	15h	16h	17h	18h	19h	20h	21h	22h	23h
0h	1h	2h	3h	4h	5h	6h	7h	8h	9h	10h	11h	12h	13h	14h	15h	16h	17h	18h	19h	20h	21h	22h	23h

BOLETIM DO ALERTA

Local: PCP Seixal
Risco: Baixo
(Previsão de 2016-01-07 00:00:00 a 2016-01-09 00:00:00)

0h	1h	2h	3h	4h	5h	6h	7h	8h	9h	10h	11h	12h	13h	14h	15h	16h	17h	18h	19h	20h	21h	22h	23h
0h	1h	2h	3h	4h	5h	6h	7h	8h	9h	10h	11h	12h	13h	14h	15h	16h	17h	18h	19h	20h	21h	22h	23h

BOLETIM DO ALERTA

Local: IH Azinheira
Risco: Sem risco
(Previsão de 2016-01-07 00:00:00 a 2016-01-09 00:00:00)

0h	1h	2h	3h	4h	5h	6h	7h	8h	9h	10h	11h	12h	13h	14h	15h	16h	17h	18h	19h	20h	21h	22h	23h
0h	1h	2h	3h	4h	5h	6h	7h	8h	9h	10h	11h	12h	13h	14h	15h	16h	17h	18h	19h	20h	21h	22h	23h

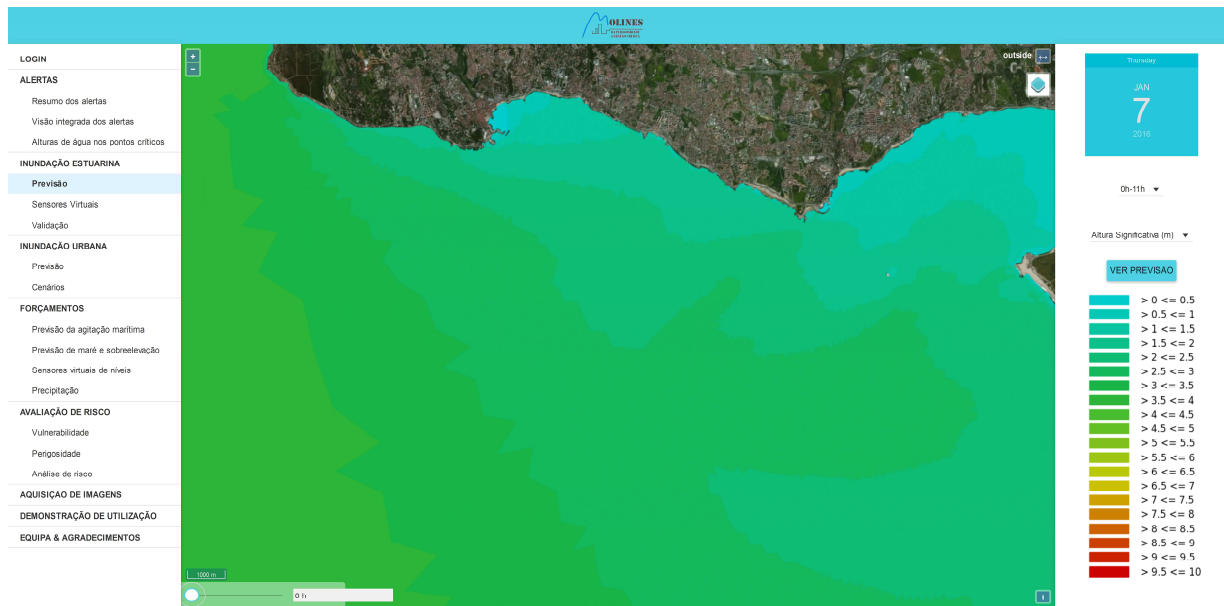
BOLETIM DO ALERTA

Local: Terminal Transtejo
Risco: Sem risco
(Previsão de 2016-01-07 00:00:00 a 2016-01-09 00:00:00)

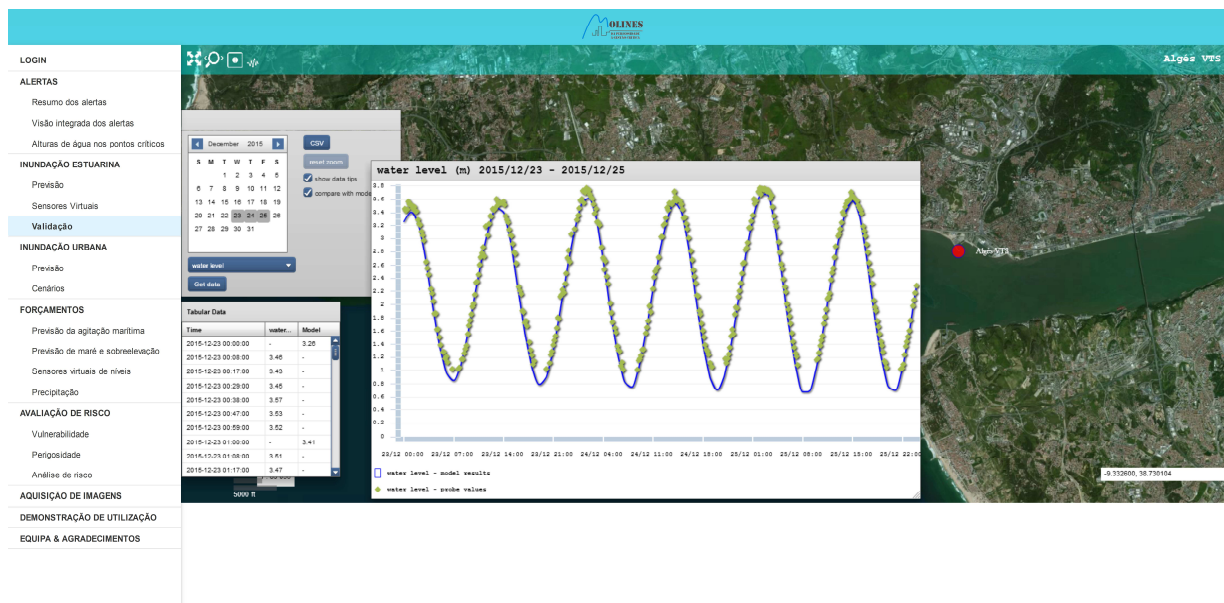
0h	1h	2h	3h	4h	5h	6h	7h	8h	9h	10h	11h	12h	13h	14h	15h	16h	17h	18h	19h	20h	21h	22h	23h
0h	1h	2h	3h	4h	5h	6h	7h	8h	9h	10h	11h	12h	13h	14h	15h	16h	17h	18h	19h	20h	21h	22h	23h

BOLETIM DO ALERTA

642



643



644

645 **Figure 9. a) General overview of the WIFF deployment for the Tagus and of its services,**
 646 **showing an integrated geographical view of the warnings for the Seixal municipality; b)**
 647 **summary of the warnings for the Seixal area, with the colored bars showing the warning**
 648 **levels at several vulnerable locations selected by the civil protection agents; c) forecast of**
 649 **the significant wave heights, in meters; d) automatic data / model comparison at the Algés**
 650 **tide gauge. The menu on the left-hand side of the figure (in Portuguese) reads: Login,**
 651 **Alerts, Estuarine inundation, Urban inundation, Forcings, Risk evaluation, Images**
 652 **acquisition, Demonstration of use, Team and acknowledgements.**